

Ambient modal identification of structures equipped with tuned mass dampers using parallel factor blind source separation

A. Sadhu^{*}, B. Hazra^a and S. Narasimhan^b

Department of Civil & Environmental Engineering, University of Waterloo, 200 University Avenue West, Waterloo, Ontario, Canada, N2L 3G1

(Received August 10, 2012, Revised June 12, 2013, Accepted June 13, 2013)

Abstract. In this paper, a novel PARAllel FACtor (PARAFAC) decomposition based Blind Source Separation (BSS) algorithm is proposed for modal identification of structures equipped with tuned mass dampers. Tuned mass dampers (TMDs) are extremely effective vibration absorbers in tall flexible structures, but prone to get de-tuned due to accidental changes in structural properties, alteration in operating conditions, and incorrect design forecasts. Presence of closely spaced modes in structures coupled with TMDs renders output-only modal identification difficult. Over the last decade, second-order BSS algorithms have shown significant promise in the area of ambient modal identification. These methods employ joint diagonalization of covariance matrices of measurements to estimate the mixing matrix (mode shape coefficients) and sources (modal responses). Recently, PARAFAC BSS model has evolved as a powerful multi-linear algebra tool for decomposing an n^{th} order tensor into a number of rank-1 tensors. This method is utilized in the context of modal identification in the present study. Covariance matrices of measurements at several lags are used to form a 3rd order tensor and then PARAFAC decomposition is employed to obtain the desired number of components, comprising of modal responses and the mixing matrix. The strong uniqueness properties of PARAFAC models enable direct source separation with fine spectral resolution even in cases where the number of sensor observations is less compared to the number of target modes, i.e., the underdetermined case. This capability is exploited to separate closely spaced modes of the TMDs using partial measurements, and subsequently to estimate modal parameters. The proposed method is validated using extensive numerical studies comprising of multi-degree-of-freedom simulation models equipped with TMDs, as well as with an experimental set-up.

Keywords: modal identification; blind source separation; parallel factor decomposition; tuned-mass damper; MTMD

1. Introduction

Blind Source Separation (BSS) methods have gained acceptance as a powerful means of ambient modal identification applicable to a large class of structural mode estimation problems (Antoni 2005, Hazra *et al.* 2010, Hazra *et al.* 2012, Sadhu *et al.* 2011, Sadhu *et al.* 2012, Sadhu *et*

*Corresponding author, Postdoctoral Fellow, E-mail: ayansadhu.civil@gmail.com

^a Postdoctoral Fellow

^b Associate Professor

et al. 2012, Yang and Nagarajaiah 2012, Sadhu and Narasimhan 2013, Abazarsa *et al.* 2013). A major application where traditional BSS methods have not been explored fully is for structural health monitoring of flexible structures equipped with tuned mass dampers (TMD). TMDs are passive vibration absorbers that suppress unwanted vibrations in flexible structures. Their dynamics and design (often called tuning) are well understood, e.g., (DenHartog 1956, Warburton 1982, Rana and Soong 1998, Gerges and Vickery 2005). Detuning, resulting from an alteration of the properties of the primary structure, deterioration of the TMD itself, in-correct design forecasts, etc., lead to a significant loss in the TMD's performance. Multiple TMDs (MTMDs) (Abe and Fujino 1994, Chen and Wu 2003, Lee *et al.* 2006), semi-active, and adaptive TMDs (Nagarajaiah 2009, Roffel *et al.* 2011, Roffel *et al.* 2013) are examples of control devices designed to overcome the problem of detuning in TMDs (Nagarajaiah and Varadarajan 2005, Kareem and Kline 1995). In order to assess the magnitude of detuning and thereby restore their optimal functionality, it is important to estimate the modal properties to which the TMD is attached to, and subsequently compare its as-built condition to the optimal performance (Hazra *et al.* 2010). However, many existing output-only algorithms encounter difficulties in achieving this objective, primarily due to the presence of closely spaced modes accompanied by a relatively high amount of damping in the fundamental mode(s) introduced by the TMD (Hazra *et al.* 2010).

Second-order Blind Identification (SOBI) (Belouchrani *et al.* 1997) and Independent Component Analysis (ICA) (Hyvarinen 1999) are the most extensively applied BSS methods for modal identification. In their basic form, both SOBI and ICA aim to estimate the modes and modal responses from a set of measurements without the knowledge of sources. This is called the static-mixtures case and forms one of the key assumptions in all BSS methods. As well, most BSS applications assume that the number of measurements is equal to, or larger than the number of sources, which are modal responses in the context of ambient modal identification, to be estimated. Recently the authors have developed new algorithms based on SOBI to handle higher damping (Hazra *et al.* 2010) (also called MCC method), second-order nonstationarity due to earthquake excitations (Sadhu *et al.* 2012), when low energy higher modes (Hazra *et al.* 2010) and narrowband excitation (Sadhu and Narasimhan 2013) are present, and when the number of sensors are less than the number of sources, i.e., underdetermined mixtures (Hazra *et al.* 2012, Sadhu *et al.* 2011, Sadhu *et al.* 2012).

Although the issue of identification in the context of TMDs has been dealt with in the literature (Lin *et al.* 2001, Hazra *et al.* 2010, Cho *et al.* 2012), a general BSS algorithm dealing with problems such as MTMDs and partial sensor measurements in noisy environments (in TMD-equipped structures) has not yet been presented. To the knowledge of the authors, identification of structures with MTMDs still remains an open problem. In their previous work (Hazra *et al.* 2010), the authors used a signal processing tool called empirical mode decomposition (EMD) to extract the intrinsic mode functions (IMFs) from measurements corresponding to the closely spaced modes. The IMFs are then used to estimate of the mode shape matrix using iterative and/or non-iterative procedures within the framework of MCC (Hazra *et al.* 2012, Hazra *et al.* 2010). However, this method is susceptible to mode-mixing due to EMD and the need of prior knowledge regarding the spectral characteristics.

PARAllel FACtor (PARAFAC) decomposition (Lathauwer 1997, Lathauwer and Castaing 2008) is a higher-order tensor modeling and decomposition tool of BSS based on multi-linear algebra with strong uniqueness properties. This tool has shown significant promise in performing source separation even with sparse measurements in a number of applications (Smilde *et al.* 2004). Several forms of PARAFAC decomposition exist in the literature (Kruskal 1977, Stegeman *et al.*

2006, Lathauwer and Castaing 2008), and our ability to harness its potential depends on the mathematical framework of the underlying problem at hand. For the case of ambient modal identification, PARAFAC decomposition can be utilized by assuming that the covariance matrices of vibration measurements at several lags can be formulated as a third-order tensor, which allows us to use PARAFAC decomposition as a powerful tool in blind modal identification. In a recent study, PARAFAC decomposition is subsequently employed in conjunction with Bayesian model updating method (Abazarsa *et al.* 2013) to estimate the modal parameters of structures. However, the separability of closely-spaced modes, low-energy modes and noise robustness of PARAFAC method was not studied in the aforementioned work. The novelty of the present work lies in overcoming the robustness issues and inaccuracies in identifying closely-spaced sources due to the presence of single or multiple TMDs in linear structures, where traditional output-only modal identification methods do not perform well (Lin *et al.* 2001, Hazra *et al.* 2010, Hazra *et al.* 2010, Cho *et al.* 2012).

The paper is organized as follows. The problem statement is presented first followed by a brief background on TMDs and PARAFAC. The general problem formulation of ambient modal identification is then presented in a BSS-PARAFAC framework. Finally, the identification results of simulation and experimental models using the proposed method are presented, followed by the main conclusions of this study.

2. Background

Before proceeding to the algorithmic details for identification, a brief background on three key aspects is first presented. They are: (i) TMD dynamics, (ii) MCC-EMD method, and (iii) PARAFAC decomposition. Item (ii) has previously been published by the authors separately (Hazra *et al.* 2012); only the key aspects are presented in this section. This method is provided to compare the performance of the method proposed in this paper with a method previously presented by the authors based on time-frequency decompositions.

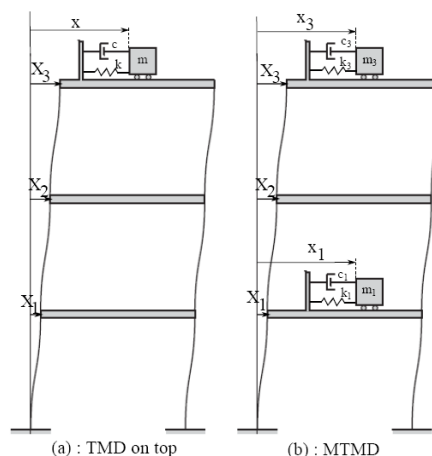


Fig. 1 Single and multiple TMDs

2.1 Dynamics of a structure with TMD

In order to understand the mechanics of TMD action, it is instructive to observe the equations of motion for a two degree-of-freedom (DOF) structural system excited by a stochastic disturbance, representing, say, wind. The equations of motion for the system in Fig. 1 can be written as

$$\begin{aligned} M\ddot{X} + C\dot{X} + KX - [k(x - X) + c(\dot{x} - \dot{X})] &= w \\ m\ddot{x} + [k(x - X_j) + c(\dot{x} - \dot{X}_j)] &= 0 \end{aligned} \quad (1)$$

where M , C , K are the mass, damping, and stiffness coefficients of the primary structure, and m , c , k are the mass, damping, and stiffness coefficients of the TMD. w is the external excitation source, which is assumed to be Gaussian and white for the purposes of this study. Of particular interest is the case of TMD for a general N -DOF primary structure. The equations of motion for the i^{th} mode when the TMD is present in the j^{th} floor level can be written as (assuming a proportionally damped system)

$$\begin{aligned} M_i\ddot{y}_i + C_i\dot{y}_i + K_i y_i - \varphi_{ij} [k(x - X_j) + c(\dot{x} - \dot{X}_j)] &= w_i \\ m\ddot{x} + [k(x - X_j) + c(\dot{x} - \dot{X}_j)] &= 0 \end{aligned} \quad (2)$$

where, the quantities M_i, C_i, K_i, w_i should be interpreted as corresponding to i^{th} mode. From Eqs. (1) and (2), one can readily observe that as long as φ_{ij} is normalized such that its value is 1 for the j^{th} location, the TMD design quantities obtained using Eq. (1) can be used directly to design a TMD corresponding to i^{th} mode (Rana and Soong 1998).

The optimal TMD parameters are specified by its optimum mass ratio (μ_{opt}), optimum frequency ratio (f_{opt}), and optimum damping ratio (ζ_{opt}). These quantities represent the ratio of the TMD parameters to the structure mass, modal frequency (to which the TMD is tuned to) and damping, respectively. Generally, μ_{opt} is assumed to be the as-built system for condition-assessment purposes, i.e., $\mu_{opt} = \mu$, the mass ratio of the existing structure. f_{opt} and ζ_{opt} are determined as a function of the mass ratio and primary structure damping ratio (ζ_p) using documented values (Rana and Soong 1998, Warburton 1982, Gerges and Vickery 2005, Lin *et al.* 2001, Hazra *et al.* 2010). In most cases, the optimal design parameters of TMD that are of practical interest are the TMD stiffness and damping k_{opt} and c_{opt} , respectively. Detuning of TMDs is mainly reflected by a reduction in the value of the TMD stiffness k_{TMD} . Thus, a parameter α is used to vary the TMD stiffness of the controlled system (i.e., $k_{TMD} = \alpha k_{opt}$) to quantify the level of de-tuning. $\alpha=1$ implies perfectly tuned condition and values less than 1 implies a detuned condition.

Multi-tuned mass dampers (MTMDs) are an extension of TMDs. They aim to improve the passive control performance of traditional TMDs either by providing optimal performance around an expected value of modal frequency (Abe and Fujino 1994, Zuo 2009), or in reducing the responses in more than one structural mode by placing them at different locations within the structure (Rana and Soong 1998). To tune a MTMD, the following design procedure is generally adopted. First, a target mass ratio contributed by n TMDs is assumed. The individual distribution of TMD masses is arrived at by estimating the peak response ratios at the corresponding locations to which the TMDs are to be placed. This is generally carried out using broadband excitations to the system. One should note that the dynamics of structural responses contain as many pairs of closely spaced modes as the number of TMDs.

2.2 Modal identification of a TMD-controlled structure using MCC-EMD

The second-order BSS techniques (e.g., MCC method) (Hazra *et al.* 2010, Hazra *et al.* 2012) are unable to resolve sources with close spectral content. In order to overcome this issue, the authors presented an algorithm where the powerful signal processing technique, EMD, is integrated within the framework of the MCC method, called the MCC-EMD method (Hazra *et al.* 2010, Hazra *et al.* 2012). EMD is a technique that reduces a signal into Intrinsic Mode Functions (IMF) that admits a Hilbert transform (Huang *et al.* 1998). For Multi-Degrees-of-Freedom (MDOF) systems, the IMFs extracted from the free-vibration responses can be regarded as the normal modes of vibration (Yang *et al.* 2003). The key idea of the MCC-EMD algorithm (for the case of a single TMD) is to separate the IMFs corresponding to the closely spaced modes using EMD, subsequently separating others using the standard MCC method, finally integrating the results.

The MCC method (Hazra *et al.* 2010) is an extension of the SOBI method (Belouchrani *et al.* 1997), which is a popular tool for BSS. For the case of static mixtures, the problem statement of BSS is given by

$$\mathbf{x}(k) = \mathbf{A}\mathbf{s}(k) \quad (3)$$

In Eq. (3), $\mathbf{A} = [a_{ij}]$ is the instantaneous mixing matrix, \mathbf{s} represents the sources. BSS methods seek \mathbf{A} and \mathbf{s} using the information contained in \mathbf{x} . Hence, the term blind is commonly used. Identifying n sources or less when the matrix \mathbf{A} is of rank n , is well-known (Kerschen *et al.* 2007, Hazra *et al.* 2010, Hazra and Narasimhan 2010).

The relationship of the MCC method with the vibration modes of a structure can be understood by examining the underlying mathematical formulation of a linear dynamic system. Consider the equations of motion for a MDOF system under the action of an excitation force vector $\mathbf{F}(\mathbf{t})$. If $\mathbf{F}(\mathbf{t})$ is assumed to be uncorrelated with one another and white, the correlation of responses $x(t)$ can be expressed in the form of Eq. 3 by the use of NExT (James *et al.* 1995)

$$R_{ijk}(T) = E[x_{ij}(t+T)x_{jk}(t)] \Leftrightarrow \mathbf{r} = \mathbf{R}(T) = \mathbf{A}_r \mathbf{s}_r \quad (4)$$

The vector \mathbf{r} contains the correlation of responses, \mathbf{s}_r is the modal response, and \mathbf{A}_r is a matrix containing the normal modes of the system (Hazra *et al.* 2010). In the above form, it is easy to recognize the similarity between Eqs. (3) and (4), provided the correlation of the responses \mathbf{r} is used in lieu of \mathbf{x} .

The key step in MCC is the simultaneous diagonalization of two covariance matrices and evaluated at zero time-lag and at some non-zero time-lag p

$$\begin{aligned} \mathbf{R}_r(0) &= E\{\mathbf{r}(k)\mathbf{r}^T(k)\} = \mathbf{A}_r \mathbf{R}_s(0) \mathbf{A}_r^T \\ \mathbf{R}_r(p) &= E\{\mathbf{r}(k)\mathbf{r}^T(k-p)\} = \mathbf{A}_r \mathbf{R}_s(p) \mathbf{A}_r^T \end{aligned} \quad (5)$$

where, $\mathbf{R}_s(p) = E\{\mathbf{s}(k)\mathbf{s}^T(k-p)\}$. With these basic definitions, the key steps are enumerated as follows (please refer to (Hazra *et al.* 2010) for details):

- Calculate the correlations of the responses to obtain the vector \mathbf{r} .
- Obtain the whitened vector $\bar{\mathbf{r}}(k) = \mathbf{Q}\mathbf{r}(k) = \mathbf{\Lambda}_r^{-\frac{1}{2}} \mathbf{V}_r^T \mathbf{r}(k)$ (where $\hat{\mathbf{R}}_r(0) = \mathbf{V}_r \mathbf{\Lambda} \mathbf{V}_r^T$)
- Divide $\mathbf{r}(k)$ into L non-overlapping blocks (time windows $T_i, i = 1, 2, 3, \dots, L$) and estimate the set of covariance matrices $\hat{\mathbf{R}}_r(T_i, p_j)$ for $i = 1, 2, 3, \dots, L$ and $j = 1, 2, 3, \dots, l$
- Find a unitary matrix that approximately diagonalizes the set of L matrices $\mathbf{V}_r \forall \hat{\mathbf{R}}_r(p)$ at

each lag, p , using joint approximate diagonalization.

- The mixing matrix is computed as $\hat{\mathbf{A}}_r = \mathbf{Q}^{-1} \mathbf{V}_{\hat{x}}$

In the MCC-EMD method, the first 2 closely spaced IMFs (Γ_i $i = 1, 2$) of the structure (corresponding to a TMD tuned to the first mode) are extracted using EMD according to

$$\ddot{x} = \sum_{i=1}^2 \Gamma_i(t) + \hat{\varepsilon}(t) \quad (6)$$

Then, the auto-correlation of Γ_1 and Γ_2 for all time-lags are calculated and represented in a vector $\tilde{\Gamma}$. Subsequently, the next $(n - 2)$ modes are extracted from the correlation of the responses (\mathbf{r}) using MCC according to

$$\begin{aligned} \hat{\mathbf{A}}_r &= \mathbf{Q}^{-1} \mathbf{V}_{\tilde{r}} \\ \tilde{\mathbf{s}} &= \hat{\mathbf{A}}_r^{-1} \mathbf{r} \end{aligned} \quad (7)$$

Then, an augmented matrix \mathbf{s}_e is constructed, expressed as

$$\mathbf{s}_e = [\tilde{\Gamma} : \tilde{\mathbf{s}}] \quad (8)$$

The modal transformation matrix, or the mixing matrix $\hat{\mathbf{A}}_e$, is estimated using the following least square estimator

$$\hat{\mathbf{A}}_e = [\mathbf{s}_e^T \mathbf{s}_e]^{-1} \mathbf{s}_e^T \mathbf{r} \quad (9)$$

The natural frequencies and the corresponding damping estimates are calculated directly by applying Hilbert transform to the recovered sources, \mathbf{s}_e .

2.3 Introduction to PARAFAC

When a signal is expressed as a multi-dimensional array, then its tensor representation allows us to use multi-linear algebra tools, which are more powerful than linear algebra tools. A vector $\mathbf{t} = t_i \in \mathfrak{R}^{n_1}$ is a first-order tensor, whereas a matrix $\mathbf{T} = t_{ij} \in \mathfrak{R}^{n_1 \times n_2}$ is second-order tensor. In general, a p -th order tensor is written as

$$\underline{\mathbf{T}} = t_{ijk \dots p} \in \mathfrak{R}^{n_1 \times n_2 \times n_3 \times \dots \times n_p} \quad (10)$$

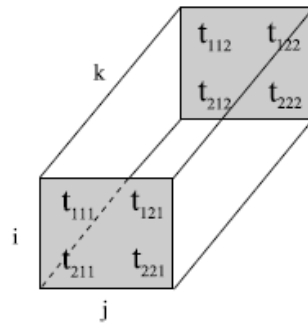


Fig. 2 Block representation of a $2 \times 2 \times 2$ tensor

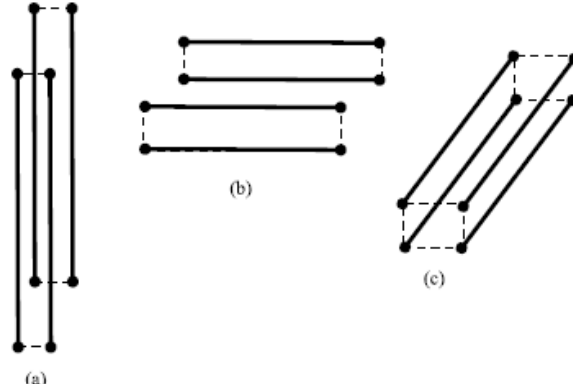


Fig. 3 Tensor fibers (a) Mode-1 fibers, (b) Mode-2 fibers, and (c) Mode-3 fibers

A 3-dimensional tensor can be visualized as a parallelepiped. The simplest 3-dimensional tensor is a $2 \times 2 \times 2$ tensor as shown in Fig. 2. Like matrices, a tensor is defined by its higher order fibres, mode-1 (column) fibres ($t_{:jk}$), mode-2 (row) fibres ($t_{i:k}$) and mode-3 (tube) fibres ($t_{ij:}$) as shown in Fig. 3. They are obtained by fixing any two of the three indices. On the other hand, if we fix any one of the indices, it results in three kinds of slices – horizontal ($t_{i::}$), lateral ($t_{:j:}$) and frontal ($t_{::k}$) which form the slices of three respective modes. For example, mode-1 slices comprise of two horizontal slices and it is described as

$$\underline{\mathbf{T}}_{(1)} = \begin{bmatrix} t_{1::} \\ t_{2::} \end{bmatrix} = \begin{bmatrix} t_{111} & t_{121} & t_{112} & t_{122} \\ t_{211} & t_{221} & t_{212} & t_{222} \end{bmatrix} \quad (11)$$

Along the same lines, mode-2 and mode-3 can be expressed as

$$\underline{\mathbf{T}}_{(2)} = \begin{bmatrix} t_{111} & t_{211} & t_{112} & t_{212} \\ t_{121} & t_{221} & t_{122} & t_{222} \end{bmatrix} \quad (12)$$

and

$$\underline{\mathbf{T}}_{(3)} = \begin{bmatrix} t_{111} & t_{121} & t_{211} & t_{221} \\ t_{112} & t_{122} & t_{212} & t_{222} \end{bmatrix} \quad (13)$$

respectively. Therefore, a tensor can be represented as a matrix by rearranging its entities, which is commonly known as matricization. Thus, Eqs. (11) - (13) are the mode-1, mode-2 and mode-3 matricizations, respectively. While considering the product of a tensor and a matrix, one has to decide which dimension of the tensor will be taken into account and this is where the matricization plays an important role. In multi-linear algebra, one decides the dimension of the tensor by defining the n -mode product of a tensor with a matrix \mathbf{A} as defined below

$$\underline{\mathbf{P}} = \underline{\mathbf{T}} \times_n \mathbf{A} \Leftrightarrow \underline{\mathbf{P}}_n = \mathbf{A} \underline{\mathbf{T}}_n \quad (14)$$

where each n -mode fibre of $\underline{\mathbf{T}}$ is multiplied by the matrix \mathbf{A} to compute n -mode fibre of the resulting tensor $\underline{\mathbf{P}}$.

A third-order tensor is primarily decomposed into a sum of outer products of triple vectors as shown in Fig. 4:

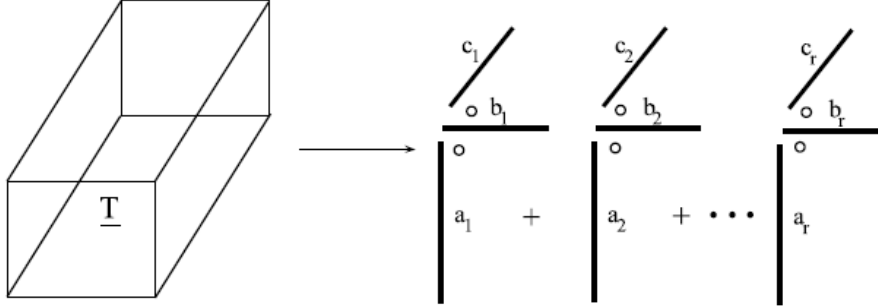


Fig. 4 Tensor decomposition

$$\underline{\mathbf{T}} = \sum_{r=1}^R \mathbf{a}_r \circ \mathbf{b}_r \circ \mathbf{c}_r \Leftrightarrow \underline{\mathbf{T}}_{ijk} = \sum_{r=1}^R a_{ir} b_{jr} c_{kr} \quad (15)$$

where $i \in [1 I]$, $j \in [1 J]$ and $k \in [1 K]$. This is also called a tri-linear model of $\underline{\mathbf{T}}$, $\underline{\mathbf{T}} = [\mathbf{A}, \mathbf{B}, \mathbf{C}]$, where the matrices are given by $\mathbf{A} = (\mathbf{a}_1, \mathbf{a}_2, \dots, \mathbf{a}_R)$, $\mathbf{B} = (\mathbf{b}_1, \mathbf{b}_2, \dots, \mathbf{b}_R)$, and $\mathbf{C} = (\mathbf{c}_1, \mathbf{c}_2, \dots, \mathbf{c}_R)$. Each triple vector product is a rank-1 tensor and is denoted as PARAFAC. Therefore, Eq. 15 represents the summation of R rank-1 tensors or PARAFAC components that are needed to fit the tensor; it is also known as the rank of the tensor $\underline{\mathbf{T}}$ (Bro 1997, Lathauwer 1997). PARAFAC components are usually estimated by minimization of the quadratic cost function

$$g(a, b, c) = \|\underline{\mathbf{T}} - \sum_{r=1}^R \mathbf{a}_r \circ \mathbf{b}_r \circ \mathbf{c}_r\|^2 \quad (16)$$

The technique was introduced simultaneously in two different independent works; canonical decomposition (CANDECOMP) (Carroll and Chang 1970) or PARALLEL FACTOR (PARAFAC) analysis (Harshman 1970). The algorithms used to fit the PARAFAC model are usually classified in three main groups: (a) alternating least squares (ALS), which updates only a subset of parameters at each step; (b) derivative-based methods; seeking an update for all the parameters simultaneously by successive approximations, and (c) direct or non-iterative approaches. Out of these, ALS method has several advantages including easier implementation, guaranteed convergence and handling capability of higher order tensors. Using ALS, one can find the PARAFAC components \mathbf{A} , \mathbf{B} and \mathbf{C} until it achieves the desired convergence

$$\begin{aligned} \mathbf{A} &\leftarrow \underline{\mathbf{T}}_{(1)}(\mathbf{C} \odot \mathbf{B})(\mathbf{C}^T \mathbf{C} * \mathbf{B}^T \mathbf{B})^\dagger \\ \mathbf{B} &\leftarrow \underline{\mathbf{T}}_{(2)}(\mathbf{C} \odot \mathbf{A})(\mathbf{C}^T \mathbf{C} * \mathbf{A}^T \mathbf{A})^\dagger \\ \mathbf{C} &\leftarrow \underline{\mathbf{T}}_{(3)}(\mathbf{B} \odot \mathbf{A})(\mathbf{B}^T \mathbf{B} * \mathbf{A}^T \mathbf{A})^\dagger \end{aligned} \quad (17)$$

where \odot indicates Khatri-Rao product. ALS is primarily consists of the following key steps which exploit the simultaneous unfolding of three matrices:

- Fix \mathbf{A} and \mathbf{B} , solve for \mathbf{C}

$$\min_{\mathbf{C}} \|\underline{\mathbf{T}} - [\mathbf{A}, \mathbf{B}, \mathbf{C}]\|^2 = \min_{\mathbf{C}} \|\underline{\mathbf{T}}_{(3)}(\mathbf{B} \odot \mathbf{A})(\mathbf{B}^T \mathbf{B} * \mathbf{A}^T \mathbf{A})^\dagger\|^2 \quad (18)$$

- Optimal \mathbf{C} is the least square solution

$$\mathbf{C} \leftarrow \underline{\mathbf{T}}_{(3)}(\mathbf{B} \circ \mathbf{A})(\mathbf{B}^T \mathbf{B} * \mathbf{A}^T \mathbf{A})^\dagger \quad (19)$$

- Successively solve for each component of \mathbf{A} , \mathbf{B} and \mathbf{C}

Finally, the algorithm tries to find a tensor $\underline{\mathbf{T}} = \sum_{r=1}^R \mathbf{a}_r \circ \mathbf{b}_r \circ \mathbf{c}_r$ such that the following expression is minimized

$$\| \underline{\mathbf{T}} - \hat{\underline{\mathbf{T}}} \|_F \quad (20)$$

where $\|\cdot\|_F$ represents the Frobenius norm. A unique decomposition is obtained if the following Kruskal condition (Kruskal 1977) is satisfied

$$k_A + k_B + k_C \geq 2R + 2 \quad (21)$$

where k_A , k_B and k_C are k -rank of the matrices \mathbf{A} , \mathbf{B} and \mathbf{C} respectively, where k -rank is defined as maximum number k such that every set of k columns of the matrix is linearly independent (Kruskal 1977).

In order to demonstrate the source separation capability of PARAFAC, three ($n_m = 3$) mixtures of four ($n_s = 4$) sine waves with frequencies 1.0, 1.1, 2.3 and 3.1 Hz are considered as shown in Eq. (22). It may be noted that the first two frequencies are closely-spaced in nature and analogous to the case of TMDs.

$$\begin{bmatrix} x_1 \\ x_2 \\ x_3 \end{bmatrix} = \begin{bmatrix} 5 & -1 & -1 & 2 \\ -1 & 3 & 1 & 2 \\ -1 & 1 & 2 & 3 \end{bmatrix} \begin{bmatrix} s_1 \\ s_2 \\ s_3 \\ s_4 \end{bmatrix} \quad (22)$$

Since the mixtures contain 4 sources, rank-4 PARAFAC decomposition is then performed to extract the hidden closely-spaced and other sources from the underdetermined mixtures. Fig. 5 shows true sources and their mixtures. Fig. 6 shows the resulting auto-correlation functions of the estimated sources $\hat{\mathbf{s}}$. PARAFAC decomposition yields \mathbf{a}_1 , \mathbf{a}_2 , \mathbf{a}_3 and \mathbf{a}_4 as shown in Fig. 6 from which the mixing matrix can be estimated by concatenating successive normalized \mathbf{a} 's

$$\begin{bmatrix} -8.44 & 1.96 & -2.2 & -3.66 \\ 1.68 & -5.88 & 2.2 & -3.66 \\ 1.68 & -1.96 & 4.4 & -5.46 \end{bmatrix} = \begin{bmatrix} 5 & -1 & -1 & 2 \\ -1 & 3 & 1 & 2 \\ -1 & 1 & 2 & 3 \end{bmatrix} \quad (23)$$

3. Details of the algorithm

Consider a linear, classically damped, and lumped-mass n_s -DOF structural system, subjected to an excitation force, $\mathbf{F}(t)$.

$$\mathbf{M}\ddot{\mathbf{x}}(t) + \mathbf{C}\dot{\mathbf{x}}(t) + \mathbf{K}\mathbf{x}(t) = \mathbf{F}(t) \quad (24)$$

where, $\mathbf{x}(t)$ is a vector of displacement coordinates at the degrees of freedom. \mathbf{M} , \mathbf{C} , and \mathbf{K} are the mass, damping and stiffness matrices of the multi-degree-of-freedom system. The solution to Eq. 24 can be written in terms of modal superposition of vibration modes with the following matrix form

$$\mathbf{x} = \Phi \mathbf{q} \quad (25)$$

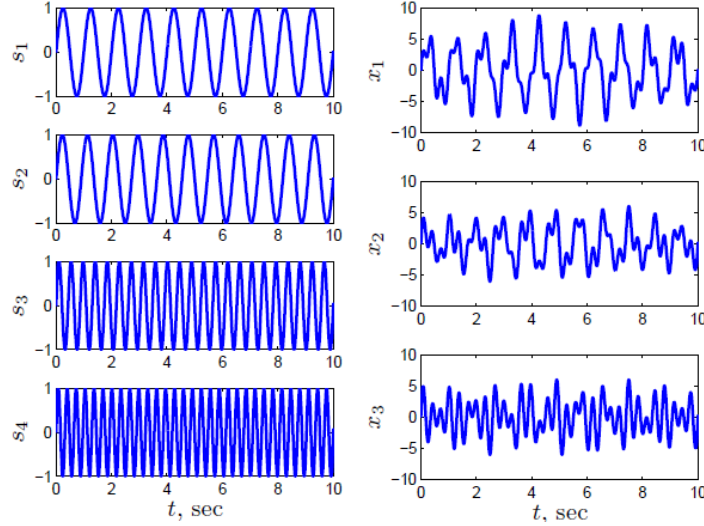


Fig. 5 Underdetermined mixtures of sine waves

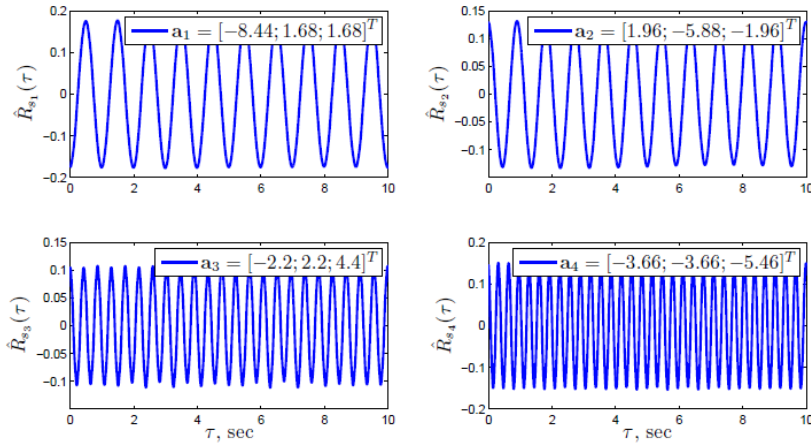


Fig. 6 Estimated sources using PARAFAC decomposition

where, $x \in \mathcal{R}^{n_m \times N}$ is the trajectory matrix composed of the sampled components of x , $q \in \mathcal{R}^{n_s \times N}$ is a matrix of the corresponding modal coordinates, $\Phi_{n_m \times n_s}$ is the modal transformation matrix, and N is the number of data points in the measurements. n_m and n_s are the number of measurements and sources respectively. The measurement at the i^{th} DOF ($i=1,2,\dots,n_m$) of Eq. (25) can be expressed as $x_i(t) = \sum_{r=1}^{n_s} \phi_{ir} q_r(t)$. Under the conditions when the modal coordinates are mutually uncorrelated with non-similar spectra, the normal coordinates can be regarded as the most uncorrelated sources. Thus, the modal coordinates \mathbf{q} are a special case of general sources \mathbf{s} with time structure, and subsequently form the basis of the BSS-based modal identification procedure described in this paper. Furthermore, the scalar multiplication for the components in \mathbf{x} is not

expected to introduce ambiguity in the process of modal identification.

Covariance matrix $\mathbf{R}_x(p_k)$ evaluated at the time-lag p_k can be written as

$$\mathbf{R}_x(p_k) = E\{\mathbf{x}(k)\mathbf{x}(n-p_k)^T\} = \mathbf{A}\mathbf{R}_s(p_k)\mathbf{A}^T \quad (26)$$

where

$$\mathbf{R}_s(p_k) = E\{\mathbf{s}(n)\mathbf{s}^T(n-p_k)\} \quad (27)$$

For notational simplicity we introduce the following definitions

$$\begin{aligned} \mathbf{R}_{x_1x_2}(p_k) &= \mathbf{R}_{12k}^x \Leftrightarrow \mathbf{R}_{x_ix_j}(p_k) = \mathbf{R}_{ijk}^x \\ \mathbf{R}_{s_1}(p_k) &= \mathbf{R}_{k1}^s \Leftrightarrow \mathbf{R}_{s_l}(p_k) = \mathbf{R}_{kl}^s \end{aligned} \quad (28)$$

Eq. (26) can be expanded for $\mathbf{x} = \{x_1, x_2, x_3\}$ as follows

$$\begin{bmatrix} R_{11k}^x & R_{12k}^x & R_{13k}^x \\ R_{21k}^x & R_{22k}^x & R_{23k}^x \\ R_{31k}^x & R_{32k}^x & R_{33k}^x \end{bmatrix} = \begin{bmatrix} a_{11} & a_{12} & a_{13} \\ a_{21} & a_{22} & a_{23} \\ a_{31} & a_{32} & a_{33} \end{bmatrix} \begin{bmatrix} \mathbf{R}_{k1}^s & 0 & 0 \\ 0 & \mathbf{R}_{k2}^s & 0 \\ 0 & 0 & \mathbf{R}_{k3}^s \end{bmatrix} \begin{bmatrix} a_{11} & a_{21} & a_{31} \\ a_{12} & a_{22} & a_{32} \\ a_{13} & a_{23} & a_{33} \end{bmatrix} \quad (29)$$

From Eq. (29), using simplified notations as in Eq. (28), $R_{x_1x_2}(p_k) = R_{12k}^x$ can be expressed as

$$R_{12k}^x = a_{11} a_{21} R_{k1}^s + a_{12} a_{22} R_{k2}^s + a_{13} a_{23} R_{k3}^s \quad (30)$$

which can be generalized for R_{ijk}^x as

$$R_{ijk}^x = a_{i1} a_{j1} R_{k1}^s + a_{i2} a_{j2} R_{k2}^s + a_{i3} a_{j3} R_{k3}^s = \sum_{r=1}^3 a_{ir} a_{jr} R_{kr}^s \quad \mathbf{i}, \mathbf{j} = 1, 2, 3; \mathbf{k} = 1, 2, \dots, p_k \quad (31)$$

For any general n_s -DOF system

$$R_{ijk}^x = \sum_{r=1}^{n_s} a_{ir} a_{jr} R_{kr}^s \Leftrightarrow \mathbf{R}^x = \sum_{r=1}^{n_s} \mathbf{a}_r \circ \mathbf{a}_r \circ R_r^s \quad (32)$$

Considering the similarity between Eqs. (15) and (32), it is seen that by decomposing the third order tensor \mathbf{R}^x into n_s rank-1 tensors, the mixing matrix can be estimated. By using PARAFAC decomposition, the resulting solutions yield the mixing matrix $\mathbf{A} = [\mathbf{a}_1, \mathbf{a}_2, \mathbf{a}_3, \dots, \mathbf{a}_{n_s}]$ and the auto-correlation function of \mathbf{R}_r^s for $r = 1, 2, 3, \dots, n_s$ from which the natural frequency and damping can be estimated, provided it is free or broadband type of excitation. Unlike a two-way array (matrix case), PARAFAC yields unique decomposition even if the rank is greater than the smallest dimension of tensor (Lathauwer and Castaing 2008). Such identifiability capability of PARAFAC is utilized in the present study for underdetermined source separation in the framework of sparse BSS. By comparing Eqs. (15) and (32), it can be concluded that Eq. (32) is a special type of PARAFAC model with $\mathbf{B}=\mathbf{A}$. Under such situations, a more relaxed uniqueness condition is proposed where the following inequality is satisfied (Stegeman *et al.* 2006).

$$\frac{n_s(n_s-1)}{2} = \frac{n_m(n_m-1)}{4} \left[\frac{n_m(n_m-1)}{2} + 1 \right] - \frac{n_m!}{(n_m-4)!4!} (n_m) \{n_m \geq 4\} \quad (33)$$

where

$$\begin{aligned} (n_m) \{n_m \geq 4\} &= 0 & n_m < 4 \\ (n_m) \{n_m \geq 4\} &= 1 & n_m \geq 4 \end{aligned} \quad (34)$$

Using Eq. (33), an upper bound of source separability of PARAFAC decomposition as in Table 1 can be computed.

Table 1 Source separation capability of PARAFAC decomposition

n_m	2	3	4	5	6	7	8	9	10
n_s	2	4	6	10	15	20	26	33	41

The key steps of the PARAFAC decomposition is summarized below:

- Obtain the partial ($n_m < n_s$) or full measurements ($n_m \geq n_s$).
- Estimate the covariance matrix $R_x(p_k)$ for a given lag p_k .
- For several lags $i = 1, 2, \dots, p_k$, form a third-order tensor R_{ijk}^x as shown in Eq. (31).
- Solve the PARAFAC model for \mathbf{R}^x to estimate \mathbf{A} and \mathbf{R}_r^s .
- Estimate natural frequencies (ω_i) and damping (ζ_i) using \mathbf{R}_r^s , and compute the mode shape matrix using \mathbf{A} .

4. Numerical study

4.1 5-DOF building with a TMD

First, simulations are performed on a 5-storey shear-beam structure model with TMD located at the roof (Hazra *et al.* 2010). The state-space model for this system subjected to an external disturbance vector \mathbf{w} is given by

$$\begin{aligned}\dot{\mathbf{x}} &= \mathbf{A}\mathbf{x} + \mathbf{E}\mathbf{w} \\ \mathbf{y} &= \tilde{\mathbf{C}}\mathbf{x}\end{aligned}\quad (35)$$

Here, the vector \mathbf{x} is a vector of states, and the vector \mathbf{y} represents the output vector, governed by $\tilde{\mathbf{C}}$ matrix. The matrix \mathbf{E} governs the location of the excitation on the structure. The system matrix \mathbf{A} is constructed using \mathbf{M} , \mathbf{C} and \mathbf{K} matrices. For the example building, the lumped weight of each floor is assumed to be 19.2 kN, and damping is assumed to be 2% critical in all modes. The natural frequencies are 0.91, 3.37, 7.11, 10.66 and 12.73 Hz. The mode shape matrix (normalized with respect to the top) for the building is given by

$$\begin{bmatrix} 1.00 & 1.00 & 1.00 & 1.00 & 1.00 \\ 0.82 & -0.087 & -1.29 & -2.52 & -3.39 \\ 0.59 & -0.91 & -0.87 & 1.81 & 5.43 \\ 0.34 & -1.02 & 1.23 & 0.94 & -5.84 \\ 0.11 & -0.48 & 1.35 & -2.86 & 4.84 \end{bmatrix}\quad (36)$$

An optimally designed TMD is placed at top floor of the 5-DOF model. The weight of TMD is 2.74 kN, $k=77.8$ N/cm, and $c=3.72$ Ns/cm (Hazra *et al.* 2010). Due to the insertion of the TMD, two closely-spaced modes at frequencies of 0.78 and 0.99 Hz appear in the proximity of the fundamental mode. The percentage of separation of the closely spaced modes (i.e., $\Delta f=0.21$ Hz)

calculated with respect to 0.99 Hz is 20%. The system is excited by the Gaussian white noise at all the floor locations.

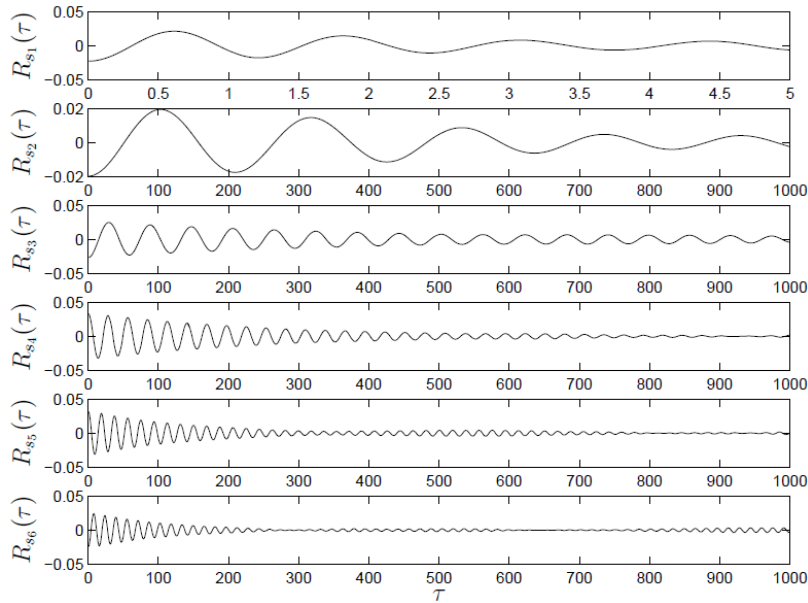


Fig. 7 5-DOF+TMD model: \mathbf{R}_r^s using PARAFAC decomposition

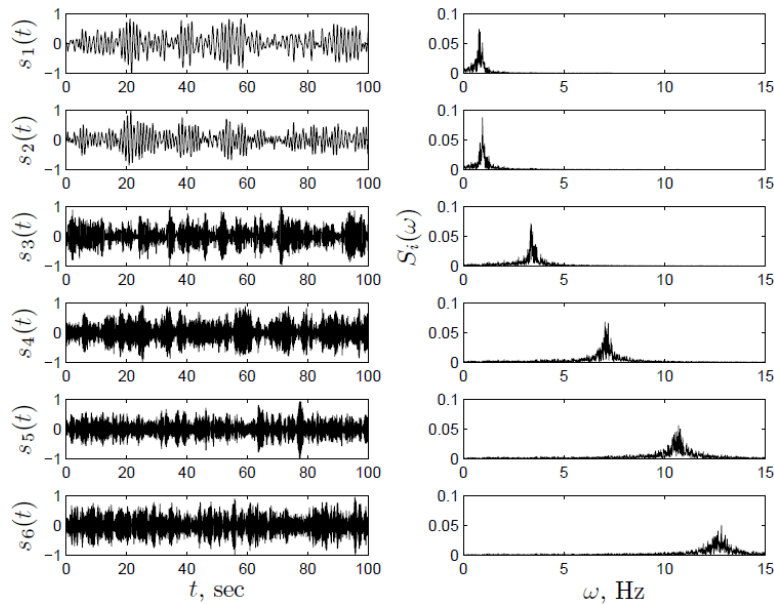


Fig. 8 5-DOF+TMD model: estimated sources and their Fourier spectra

The PARAFAC decomposition is then undertaken for 6 components. The resulting mixing matrix shows an average MAC (Maia and Silva 1997) number of 0.99 and the auto-correlation of the sources obtained are shown in Fig. 7, from which the natural frequency and damping can be obtained. The sources are estimated by multiplying the pseudo-inverse of the mixing matrix with the response and are shown in Fig. 8. According to Table 1, a maximum six sources can be identified using 4 sensors, and therefore similar results are obtained when the floor response of the top 4 floors are used. In this particular case, PARAFAC yields auto-correlations of 6 sources and a 4x6 mode shape matrix. Therefore, the MAC number is computed with reference to mode-shape coordinates of the true and estimated mode shape matrices corresponding to partial measurements.

The mode-shape identification results for the partial measurement case (1 – 3 – 5 – 6) is also shown in Table 2 and compared with the full sensor cases for different noise conditions with signal-to-noise ratio (SNR) of 100 and 10. It is observed that the relative MAC numbers decreases for the third and sixth modes under the higher noise level case, due to the low energy of the respective modes in the floor responses. Details of the estimated modal parameters are presented in Table 5.

Table 2 Details of the identification results of 5-DOF building with TMD

Mode	PARAFAC (SNR=100)			PARAFAC (SNR=10)		
	$n_m=6$	$n_m=5$	$n_m=4$	$n_m=6$	$n_m=5$	$n_m=4$
1	0.98	0.98	0.97	0.98	0.97	0.97
2	0.99	0.99	0.98	0.99	0.98	0.97
3	0.99	0.98	0.98	0.97	0.96	0.94
4	0.99	0.99	0.99	0.99	0.99	0.98
5	0.99	0.99	0.99	0.99	0.99	0.98
6	0.99	0.99	0.98	0.98	0.96	0.95

4.2 3-DOF building with single and multiple TMDs

In the previous example, the resolution of source separation is considered reasonably high with a value of 20%. In this example, we make an attempt to explore the extent of source separation capability of PARAFAC decomposition and compare the identification results with the MCC-EMD method. A 3-DOF model (Rana and Soong 1998) is considered as a test-bed for single-mode and multiple-mode TMDs. Readers are referred elsewhere (Rana and Soong 1998) for the details of the mass, stiffness and damping matrices. The natural frequencies of the 3-DOF primary structures are 0.71, 1.98 and 2.87 Hz, and the associated damping is assumed to be 2.0%, 0.5% and 0.3%, respectively. With the introduction of two optimally tuned TMDs, the resulting frequencies are 0.64, 0.75, 1.91, 2.04 and 2.87 Hz with damping ratios 6.3%, 5.8%, 2.2%, 2.1% and 0.3%, respectively in the corresponding modes. It may be noted that the issue associated with the optimal design of TMDs (Hazra *et al.* 2010, Roffel *et al.* 2013) is beyond the scope of the current study, and therefore is not discussed here. The frequency separation for two consecutive modes is 14.7%

and 6.4% respectively, which is relatively small. Fig. 9 (left sub-figure) shows the Fourier spectrum of the top floor response with and without the MTMD. For all the subsequent analysis pertaining to the 3-DOF model, the excitation is assumed to be Gaussian and white.

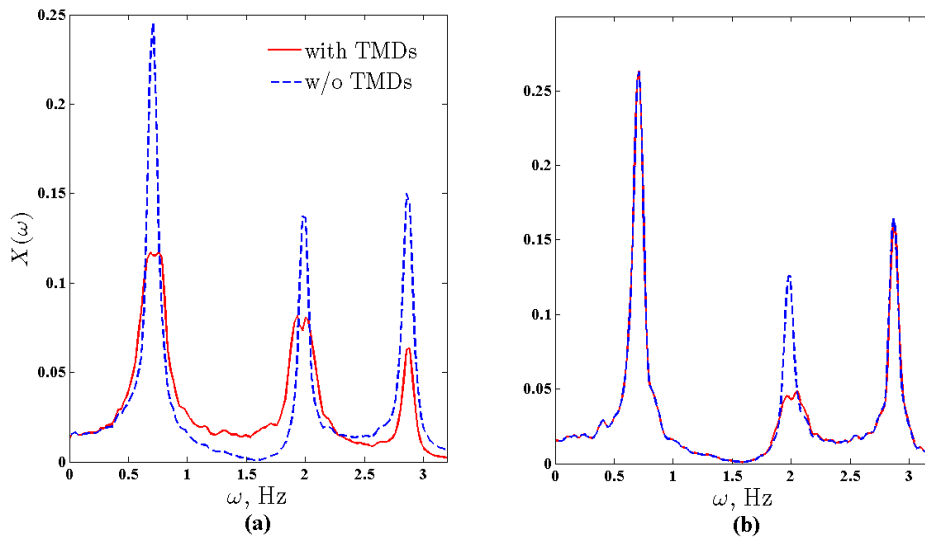


Fig. 9 3-DOF model with (a) multiple TMDs and (b) single TMD: Fourier spectrum of the top floor response

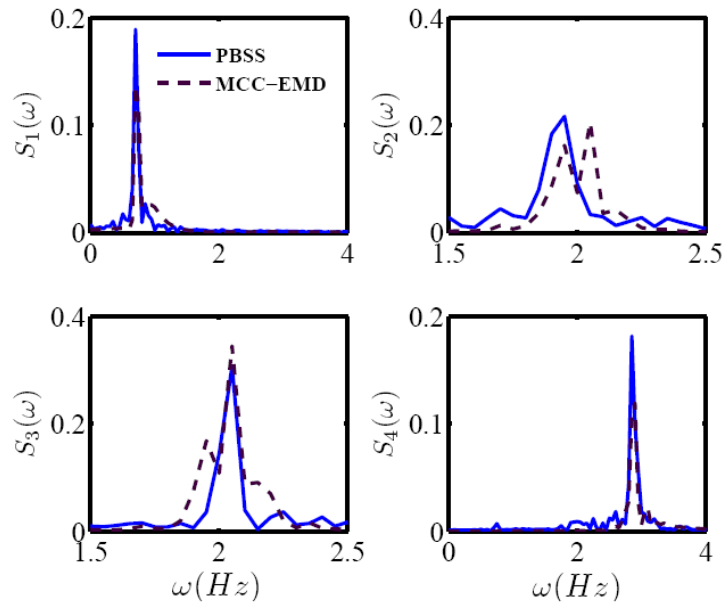


Fig. 10 Fourier spectra of the estimated sources for single TMD case

Let us consider the case where the 3-DOF model is tuned to the 2nd structural mode (i.e., with lowest frequency resolution of 6.7%). Thus, a pair of closely spaced modes at 1.91 Hz and 2.04 Hz is introduced. Fig. 9 (right sub-figure) shows 2 closely spaced peaks around 2 Hz, which corresponds to the 2nd mode tuning. The sources identified using rank-4 PARAFAC decomposition is shown in Fig. 10. From Fig. 10, it is evident that PARAFAC decomposition separates the closely spaced modes very clearly; however, the results from MCC-EMD are less reliable. However, in the previous case of 5-DOF+TMD system, MCC-EMD method was clearly able to separate the closely spaced modes (refer to (Hazra et al. 2010) for the results) where the percentage separation of the frequencies was of the order of 20%. Based on this study, it is concluded that PARAFAC decomposition is able to resolve frequency separation as low as 7%.

4.3 3-DOF with MTMD (2 TMDs)

In this case, both the TMDs are assumed to be active (see Fig. 9 (left sub-figure)). Hence, the PARAFAC decomposition is performed for 5 components using five response measurements (three floor measurements and two TMD responses). The resulting sources and their Fourier spectra are shown in Fig. 11. Table 3 shows the relative performance of PARAFAC decomposition versus MCC-EMD method. It is seen that the presence of two successive pairs of closely-spaced modes with low frequency resolution (<10%) significantly affects the performance of MCC-EMD method. On the other hand, PARAFAC decomposition results in reliable estimates (with MAC numbers greater than 0.98) even in the case of 4 sensor measurements. Details of the estimated modal parameters are reported in Table 5.

Table 3 MAC numbers of mode shapes of the 3-DOF building model with MTMD

Mode	PARAFAC		MCC-EMD	
	$n_m=5$	$n_m=4$	$n_m=5$	$n_m=4$
1	0.98	0.98	0.95	0.94
2	0.99	0.98	0.96	0.95
3	0.99	0.98	0.89	0.85
4	0.99	0.99	0.91	0.89
5	0.99	0.99	0.97	0.96

4.4 10-DOF building with a TMD

In order to demonstrate the performance of PARAFAC decomposition under partial measurements, a high-rise building model with 10 DOFs (Au *et al.* 1999) is considered. The lumped mass at all the floors are $m_i = 1 \times 10^5$ kg, $i = 1, 2, \dots, 10$. The inter-story stiffness of all the floors are assumed to be $k_i = 180 \times 10^6$ N/m. The mass of the TMD is 1% of the entire mass of the building (Au *et al.* 1999). Fourier spectra of typical floor responses are shown in Fig. 12, which clearly indicates the presence of 6 dominant modes within the frequency range of 1-10 Hz. The modes above the first 6 have little or no energy content. Therefore, rank-6 PARAFAC decomposition is used to extract first 6 PARAFAC components to identify the associated modal information.

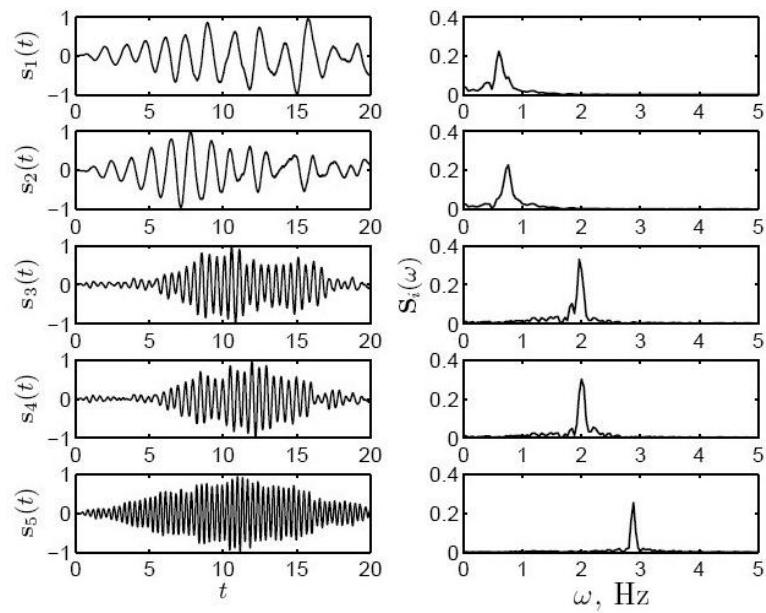


Fig. 11 3-DOF model with multiple TMDs: Estimated source and their Fourier spectrum

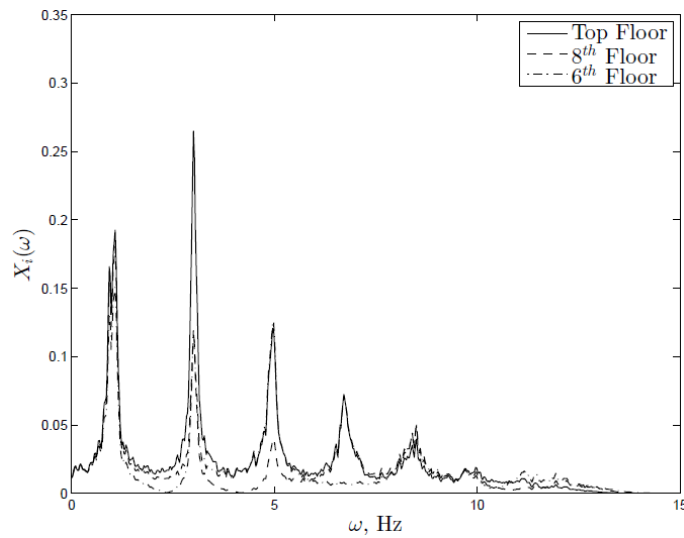


Fig. 12 10-DOF building: Fourier spectra of typical floor responses

According to Table 1, one needs 4 sensors to identify 6 PARAFAC components. Therefore, the possible number of minimal sensor configurations is ${}^{11}C_4 = 330$. However, it is seen that the identifiability criteria is dependent not only on the number of partial measurements, but also on the energy distribution of the key modes amongst those sensors. Sensors corresponding to responses with low energy content in the key modes yield poor source separation, a problem that is more

acute for the case of substantial measurement noise. Therefore, a suitable choice of sensor configuration is extremely crucial in identifying low-energy modes under the partial measurement case. A summary of average MAC numbers for the first six modes using the best (w.r.t. frequency estimates) partial sensor configuration (1 – 2 – 7 – 8) out of 330 combinations are shown in Table 4.

Table 4 MAC numbers of identified mode shapes of 10-DOF building with TMD

Mode	Full measurement ($n_m=11$)		Partial measurement ($n_m=4$)	
	SNR=100	SNR=10	SNR=100	SNR=10
1	0.99	0.99	0.99	0.96
2	1.00	0.99	0.98	0.97
3	0.99	0.98	0.99	0.99
4	0.99	0.98	0.98	0.96
5	0.99	0.91	0.97	0.89
6	0.99	0.97	0.99	0.95

Table 5 Summary of the estimated natural frequency (ω) and damping (ξ) of the numerical models using partial measurements ($n_m = 4$)

Mode	5-DOF+TMD		3-DOF+2-TMD		10-DOF+TMD (330 combinations)	
	ω (Hz)	ξ (%)	ω (Hz)	ξ (%)	μ_ω (Hz), c_v (%)	μ_ξ (%), c_v (%)
1	0.77 [0.78]*	7.8 [7.67]	0.64 [0.64]	6.7 [6.3]	0.9 [0.92], (3.3)	4.8 [4.5], (4.2)
2	1.0 [0.99]	7.1 [7.2]	0.74 [0.75]	6.1 [5.8]	1.2 [1.06], (6.8)	3.8 [3.6], (5.6)
3	3.37 [3.37]	2.06 [2.16]	1.92 [1.91]	2.3 [2.2]	2.9 [3.0], (3.4)	0.99 [1.1], (4.9)
4	7.10 [7.11]	2.0 [2.03]	2.02 [2.04]	1.9 [2.1]	4.87 [4.94], (2.1)	1.31 [1.4], (7.1)
5	10.66 [10.66]	1.98 [2.0]	2.88 [2.87]	0.5 [0.3]	6.52 [6.75], (4.8)	1.71 [1.8], (7.5)
6	12.71 [12.73]	1.98 [2.0]	–	–	8.25[8.42], (5.9)	2.04 [2.2], (6.1)

[]* represents true value

The resulting sources are shown in Fig. 13 from which the frequencies of the sources are estimated with significant accuracy (exact values are tabulated in Table 5). Detailed statistics including the mean value (μ) and coefficient of variation (c_v) of the estimated frequencies and damping are shown in Table 5 that are obtained using 330 setups of partial measurements. Relatively higher error (c_v) is observed in the estimation of damping, this is perhaps due to estimation error associated with the damping estimation from the forced vibration data (Yang *et al.*

2003, Hazra *et al.* 2010, Sadhu *et al.* 2011, Abazarsa *et al.* 2013). It can also be concluded that the performance of the PARAFAC method is sensitive to the chosen sensor configuration (Abazarsa *et al.* 2013), therefore the choice of key sensor configuration (i.e., containing higher participation of relevant structural modes) is crucial.

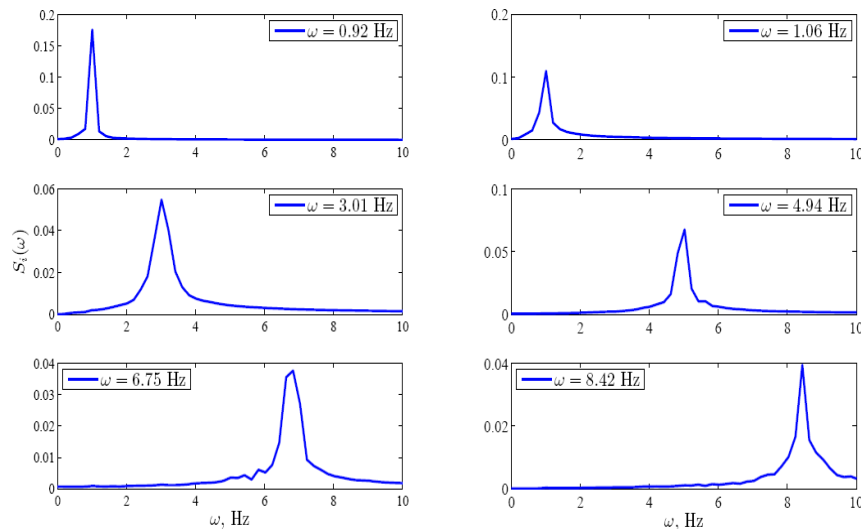


Fig. 13 Fourier spectra of auto-correlation functions of identified sources of 10-DOF+TMD building using best sensor configuration (1 – 2 – 7 – 8)

5. Experimental study

In order to demonstrate the practical applicability of the proposed identification method, the algorithm is implemented using acceleration data acquired from a bench-scale two-storey model with a pendulum TMD as shown in Fig. 14. The structural model consists of two floor weights, 140 N each. Flexural stiffness is provided by four 1.30 cm aluminum equal angles, 130 cm tall and 0.17 cm thick. The lateral frequencies of the primary system without TMD are calculated as 2.6 and 3.5 Hz. The identified structural damping in both the lateral directions is approximately 2% critical. The suspended mass is 1.5 kg, which corresponds to a mass ratio of approximately 5%. The position of a tuning frame sliding inside a rail provides a simple means to adjust the natural frequency of the pendulum. An air-damper is connected between the suspended mass and the rail assembly to provide a small amount of damping to the pendulum TMD. A broad-band excitation is commanded to an actuator (shaker shown in Fig. 14) connected to the first floor level, and the accelerations are recorded using low-frequency accelerometers at the floor levels, in both lateral directions. The theoretically calculated optimal length of the pendulum for the setup in Fig. 14 using the expressions given in the author's previous work (Hazra *et al.* 2010) is 44 mm. The sampling frequency is set to 100 Hz.

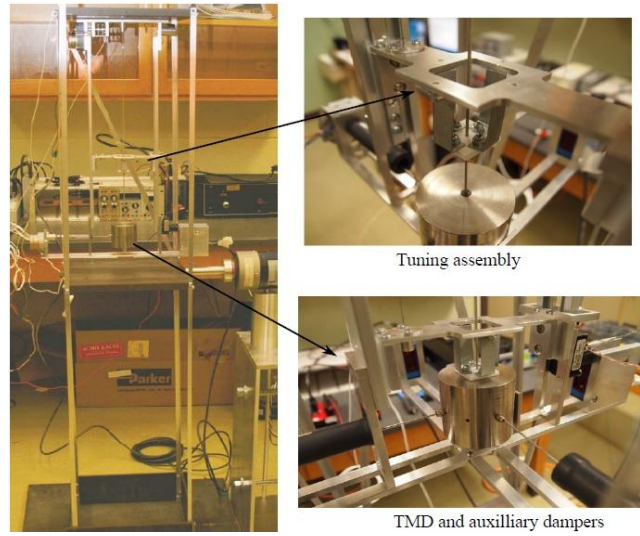


Fig. 14 Experimental setup

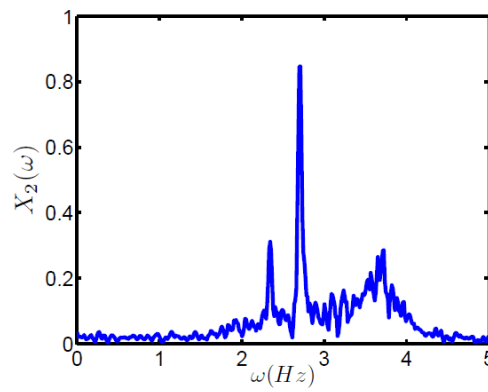


Fig. 15 Fourier spectrum of the response

Table 6 Modal identification of the experimental model

Mode	Identified frequency (Hz) using PARAFAC	Identified frequency (Hz) using MCC-EMD	Identified frequency (Hz) using SSI	MAC (PARAFAC/MCC-EMD)	MAC (SSI/MCC-EMD)
1	2.35	2.34	2.40	0.99	0.98
2	2.70	2.69	2.42	0.99	0.81
3	3.50	3.51	3.51	0.99	0.99

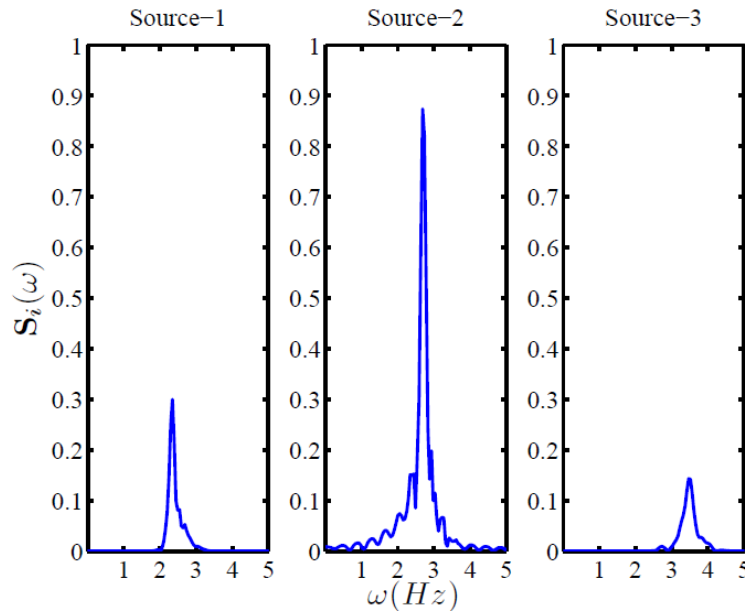


Fig. 16 Fourier spectra of the modal responses (sources)

The Fourier spectrum of the recorded response of the second floor is shown in Fig. 15. The recorded acceleration responses are processed using PARAFAC decomposition, MCC-EMD (Hazra *et al.* 2010) method and SSI method (VanOverschee and De Moor 1996) without performing any processing on the data (such as de-noising, etc.). The identified modal responses (i.e. the separated sources) obtained using PARAFAC decomposition is shown in Fig. 16. The first 2 sources correspond to the closely spaced modes of the experimental model. The results of the identification are presented in Table 6. The MAC numbers comparing the 3 methods show that the quality of identification is comparable in PARAFAC decomposition and MCC-EMD methods. The identified frequencies correspond well with the peaks in the spectral estimate as shown in Fig. 16. SSI is able to capture 2 modes only and it is very clear that it fails to resolve the closely spaced modes. This shows that PARAFAC decomposition is well equipped to handle practical measurement data.

6. Conclusions

A novel PARAFAC-decomposition based BSS method is undertaken for the modal identification of structures equipped with TMDs. The finer spectral resolution capability and identifiability property of PARAFAC are utilized to separate closely-spaced modes under the presence of partial measurements. Using an extensive numerical and experimental study, it is shown that PARAFAC decomposition is able to separate and identify closely-spaced modes with a frequency of separation as close as 7%. This method also eliminates the use of expensive and resource-consuming band-pass filtering based intermittency criteria as used in MCC-EMD method, which proves to be effective under the presence of multiple TMDs. Thus, the method promises to

be a strong candidate for separating closely spaced modes in MTMD identification problems. The study however shows that the performance of PARAFAC decomposition is significantly affected by the presence of measurement noise while using the partial measurements, an issue that remains to be addressed in future works. Furthermore, the choice of sensor configuration also needs to be investigated with the framework of PARAFAC decomposition.

References

- Abazarsa, F., Ghahari, S.F., Nateghi, F. and Taciroglu, E. (2013), "Response-only modal identification of structures using limited sensors", *Struct. Control Health Monit.*, **20**(6), 987-1006.
- Abe, M. and Fujino, Y. (1994), "Dynamic characterization of multiple tuned mass dampers and some design formulas", *Earthq. Eng. Struct. D.*, **23**, 813-835.
- Antoni, J. (2005), "Blind separation of vibration components: Principles and demonstrations", *Mech. Syst. Signal Pr.*, **19**, 1166-1180.
- Au, S.K., Papadimitriou, C. and Beck, J.L. (1999), "Reliability of uncertain dynamical systems with multiple design points", *Struct. Saf.*, **21**, 113-133.
- Belouchrani, A., Abed-Meraim, K., Cardoso, J. and Moulines, E. (1997), "A blind source separation technique using second-order statistics", *IEEE T. Signal Process.*, **45**(2), 434-444.
- Bro, R. (1997), *Parafac. tutorial and applications*, Chemometrics and Intelligent Laboratory Systems, San Antonio, Texas, February 7-10.
- Carroll, J.D. and Chang, J.J. (1970), "Analysis of individual differences in multidimensional scaling via an n-way generalization of eckart-young decomposition", *Psychometrika*, **35**(3), 283-319.
- Chen, G. and Wu, J. (2003), "Experimental study on multiple tuned mass dampers to reduce seismic responses of a three-storey building structure", *Earthq. Eng. Struct. D.*, **32**(5), 793-810.
- Cho, B.H., Jo, J.S., Joo, S.J. and Hongjin, K. (2012), "Dynamic parameter identification of secondary mass dampers based on full-scale tests", *Comput. - Aided Civ. Inf.*, **27**(3), 218-230.
- DenHartog, J. (1956), *Mechanical vibration*, McGraw-Hill, New York.
- Gerges, R. and Vickery, B. (2005), "Optimum design of pendulum-type tuned mass dampers", *Struct. Des. Tall Spec.*, **14**(4), 353-368.
- Harshman, R.A. (1970), *Foundations of the parafac procedure: Models and conditions for an explanatory multi-model factor analysis*, UCLA working papers in Phonetics.
- Hazra, B. and Narasimhan, S. (2010), "Wavelet-based blind identification of the UCLA Factor building using ambient and earthquake responses", *Smart Mater. Struct.*, **19**(2), 025005.
- Hazra, B., Roffel, A.J., Narasimhan, S. and Pandey, M.D. (2010), "Modified cross-correlation method for the blind identification of structures", *J. Eng. Mech. - ASCE*, **136**(7), 889-897.
- Hazra, B., Sadhu, A., Lourenco, R. and Narasimhan, S. (2010), "Retuning tuned mass dampers using ambient vibration response", *Smart Mater. Struct.*, **19**(11), 115002.
- Hazra, B., Sadhu, A., Roffel, A.J. and Narasimhan, S. (2012), "Hybrid time-frequency blind source separation towards ambient system identification of structures", *Comput.- Aided Civ. Inf.*, **27**(5), 314-332.
- Hazra, B., Sadhu, A., Roffel, A.J., Paquet, P.E. and Narasimhan, S. (2012), "Underdetermined blind identification of structure by using the modified cross-correlation method", *J. Eng. Mech. - ASCE*, **138**(4), 327-337.
- Huang, N.E., Shen, Z., Long, S.R., Wu, M.C., Shih, H.H., Zheng, Q., Yen, N.C., Tung, C.C. and Liu, H.H. (1998), "The empirical mode decomposition for the Hilbert spectrum for nonlinear and non-stationary time series analysis", *P. Roy. Soc. London*, 903-995.
- Hyvarinen, A. (1999), "Fast and robust fixed-point algorithm for independent component analysis", *IEEE T. Neural Networ.*, **10**(3), 626-634.
- James, G., Carne, T. and Lauffer, J. (1995), "The natural excitation technique (NExT) for modal parameter extraction from operating structures", *Modal Anal.*, **10**(4), 260-277.

- Kareem, A. and Kline, S. (1995), "Performance of multiple mass dampers under random loading", *J. Struct. Eng. - ASCE*, **121**(2), 348-361.
- Kerschen, G., Poncelet, F. and Golinval, J. (2007), "Physical interpretation of independent component analysis in structural dynamics", *Mech. Syst. Signal Pr.*, **21**(4), 1561-1575.
- Kruskal, J.B. (1977), "Three-way arrays: rank and uniqueness of trilinear decompositions with applications to arithmetic complexity and statistics", *Linear Algebra Appl.*, **18**, 95-138.
- Lathauwer, L.D. (1997), *Signal processing based on multilinear algebra*, PhD thesis, K.U. Leuven, E.E. Dept., Belgium.
- Lathauwer, L.D. and Castaing, J. (2008), "Blind identification of underdetermined mixtures by simultaneous matrix diagonalization", *IEEE T. Signal Proces.*, **56**(3), 1096-1105.
- Lee, C.L., Chen, Y.T., Chung, L.L. and Wang, Y.P. (2006), "Optimal design theories and applications of tuned mass dampers", *Eng. Struct.*, **28**(1), 43-53.
- Lin, C.C., Wang, J.F. and Ueng, J. (2001), "Vibration control identification of seismically excited m.d.o.f. structure-ptmd systems", *J. Sound Vib.*, **240**(1), 87-115.
- Maia, N.M.M. and Silva, J.M.M. (1997), *Theoretical and experimental modal analysis*, Research Studies Press, UK.
- Nagarajaiah, S. (2009), "Adaptive passive, semiactive, smart tuned mass dampers: identification and control using empirical mode decomposition, Hilbert transform, and short-term Fourier transform", *Struct. Control Health Monit.*, **16**(7-8), 800-841.
- Nagarajaiah, S. and Varadarajan, N. (2005), "Semi-active control of wind excited building with variable stiffness tmd using short-time fourier transform", *J. Eng. Struct.*, **27**(3), 431-441.
- Rana, R. and Soong, T.T. (1998), "Parametric study and simplified design of tuned mass dampers", *Eng. Struct.*, **20**(3), 193-204.
- Roffel, A., Lourenco, R., Narasimhan, S. and Yarusevych, S. (2011), "Adaptive compensation for detuning in pendulum tuned mass dampers", *J. Struct. Eng. - ASCE*, **137**(2), 242-251.
- Roffel, A., Narasimhan, S. and Haskett, T. (2013), "Performance of pendulum tuned mass dampers in reducing the responses of flexible structures", *J. Struct. Eng. - ASCE*, **139**(12), 04013019.
- Sadhu, A., Hazra, B. and Narasimhan, S. (2012), "Blind identification of earthquake-excited structures", *Smart Mater. Struct.*, **21**(4), 045019.
- Sadhu, A., Hazra, B., Narasimhan, S. and Pandey, M.D. (2011), "Decentralized modal identification using sparse blind source separation", *Smart Mater. Struct.*, **20**(12), 125009.
- Sadhu, A., Hu, B. and Narasimhan, S. (2012), "Blind source separation towards decentralized modal identification using compressive sampling", *Proceedings of the 11th International IEEE Conference on Information Science, Signal Processing and their Applications: Special Sessions*, Montreal, Canada.
- Sadhu, A. and Narasimhan, S. (2013), "A decentralized blind source separation algorithm for ambient modal identification in the presence of narrowband disturbances", *Struct. Control Health Monit.*, DOI: 10.1002/stc.1558.
- Smilde, A., Bro, R. and Geladi, P. (2004), *Multi-way Analysis with applications in the Chemical Sciences*, John Wiley and Sons, Ltd, West Sussex, UK.
- Stegeman, A., Berge, T. and Lathauwer, D. (2006), "Sufficient conditions for uniqueness in candecomp/parafac and indscal with random component matrices", *Psychometrika*, **71**(2), 219-229.
- VanOverschee, P. and De Moor, B. (1996), *Subspace identification for linear systems: theory, Implementation, Applications*. Dordrecht, Netherlands.
- Warburton, G.W. (1982), "Optimum absorber parameters for various combinations of response and excitation parameters", *Earthq. Eng. Struct. D.*, **10**(3), 381-401.
- Yang, J.N., Lei, Y., Pan, S. and Huang, N. (2003), "System identification of linear structures based on Hilbert Huang spectral analysis. part 1: normal modes", *Earthq. Eng. Struct. D.*, **32**(9), 1443-1467.
- Yang, Y. and Nagarajaiah, S. (2012), "Time-frequency blind source separation using independent component analysis for output-only modal identification of highly-damped structures", *J. Struct. Eng. - ASCE*, **139**, 1780-1793.

Zuo, L. (2009), "Effective and robust vibration control using series multiple tuned-mass dampers", *J. Vib. Acoust.*, **13**(031003), 3-11.